

neighbors with opposite orientations of their dipoles. This strong dipolar coupling explains the high degree of order in the structure.

The thermal motion of the anion atoms is relatively large; two equatorial oxygens and the axial oxygen have extremely large rms amplitudes of vibration. The other oxygen,  $\text{O}_2$ , is involved in a very close-packing interaction with  $\text{O}_2$  of the inversion-related anion at 3.504 (11) Å. Presumably this interaction constrains this oxygen somewhat while the other oxygens are able to vibrate freely in the holes created by the bulky cation. Large isotropic thermal motion for carbonyl oxygens has also been reported in a structure of the PPN cation with  $\text{Cr}_2(\text{CO})_{10}\text{I}^-$ .<sup>39</sup>

In a trigonal-bipyramidal complex of symmetry  $D_{3h}$ , the d orbitals split into the irreducible representations  $a_1'(d_z^2)$ ,  $e'(d_{x^2-y^2}, d_{xy})$ , and  $e''(d_{xz}, d_{yz})$ . Only the  $e'$  and  $e''$  orbitals are of the proper symmetry to participate in metal-to-ligand  $\pi$  bonding. For the axial ligands only the  $e''$  orbitals are available for  $\pi$  bonding. For the equatorial ligands both the  $e'$  and  $e''$  sets are available. This simple analysis leads to the expectation that (in the absence of overwhelming countereffects such as strong steric repulsion) the more strongly  $\pi$ -bonding ligands should preferentially occupy equatorial positions. The isoelectronic series of which  $\text{Fe}(\text{CO})_5$  is the parent compound is an especially good test of this hypothesis. Since  $\text{NO}^+$  is a stronger  $\pi$ -bonding ligand

than  $\text{CO}$ ,  $\text{Mn}(\text{NO})(\text{CO})_4$  should have the nitrosyl in the equatorial position, as observed.<sup>8</sup> Since  $\text{CN}^-$  is a weaker  $\pi$ -bonding ligand than  $\text{CO}$ ,  $[\text{Fe}(\text{CO})_4\text{CN}]^-$  should have the cyanide in the axial position, as this structure establishes. Other complexes which are not strictly isoelectronic are also expected to show this trend. Thus  $[\text{Fe}(\text{CO})_4\text{H}]^-$  would be expected to have the hydride in the axial position, as has been observed.<sup>38</sup>

**Acknowledgment.** We thank Mr. Richard F. Trecartin for preparing the crystalline materials used in this study. We gratefully acknowledge the financial support of the National Science Foundation (through Grant GP-29764). We thank the University of California Computing Center for the use of subsidized computer time.

**Registry No.** [PPN][ $\text{Fe}(\text{CO})_4\text{CN}$ ], 49792-33-8.

**Supplementary Material Available.** A listing of structure factor amplitudes will appear following these pages in the microfilm edition of this volume of the journal. Photocopies of the supplementary material from this paper only or microfiche (105 × 148 mm, 24 × reduction, negatives) containing all of the supplementary material for the papers in this issue may be obtained from the Journals Department, American Chemical Society, 1155 16th St., N.W., Washington, D. C. 20036. Remit check or money order for \$3.00 for photocopy or \$2.00 for microfiche, referring to code number INORG-74-770.

Contribution from Lawrence Berkeley Laboratory and Department of Chemistry, University of California, Berkeley, California 94720

## Crystal Structure of $\text{Xe}_2\text{F}_{11}^+\text{AuF}_6^-$ and the Raman Spectrum of $\text{Xe}_2\text{F}_{11}^+$

KEVIN LEARY, ALLAN ZALKIN, and NEIL BARTLETT\*

Received January 29, 1973

Crystals of  $\text{Xe}_2\text{F}_{11}^+\text{AuF}_6^-$  are orthorhombic with  $a = 9.115$  (6) Å,  $b = 8.542$  (25) Å,  $c = 15.726$  (20) Å,  $V = 1224$  Å<sup>3</sup>,  $Z = 4$ ,  $d_c = 4.24$  g cm<sup>-3</sup>, and space group  $Pnma$ . A structure determination using three-dimensional Mo  $K\alpha$  X-ray data resulted in a conventional  $R$  factor of 0.036 for 862 independent reflections for which  $I \geq 3\sigma(I)$  ( $R = 0.052$  for the 1140 independent data, including zero weight data). The anion is essentially octahedral, with an average Au-F bond distance of 1.86 (1) Å. The  $\text{Xe}_2\text{F}_{11}^+$  consists of two crystallographically independent  $\text{XeF}_5^+$  groups bridged by a common fluorine atom, with a bridge angle of 169.2 (2)°; the bridge bond lengths are 2.23 Å (average) vs. 1.84 Å (average) for the other Xe-F distances. Each  $\text{XeF}_5^+$  group departs significantly from the ideal  $C_{4v}$  symmetry of the  $\text{XeF}_5^+$  cation. However, the  $F_{ax}\text{-Xe-F}_{eq}$  angles are ~80° for both  $\text{XeF}_5^+$  and the  $\text{XeF}_5^+$  groups in  $\text{Xe}_2\text{F}_{11}^+$ . The cis angle furthest from the bridging fluorine atom is larger than the others indicating that the bridging F atom may be deflecting the nonbonding Xe(VI) valence electron pair from its ideal position in each pseudooctahedral,  $\text{XeF}_5^+$ -like component of  $\text{Xe}_2\text{F}_{11}^+$ . Raman data indicate that the complex cation behaves vibrationally like two weakly coupled  $\text{XeF}_5^+$  species with a "bridge stretch" at ~360 cm<sup>-1</sup>. This and the structural data indicate that  $F_5\text{Xe}^+\text{F-XeF}_5^+$  must be a major canonical form in the resonance hybrid description of the cation.

### Introduction

Recently we set out to synthesize  $\text{AuF}_6^-$  and obtained<sup>1</sup> our first salt of this anion in the form of the complex cation salt  $\text{Xe}_2\text{F}_{11}^+\text{AuF}_6^-$ . Since both ions were novel and of structural interest, we were fortunate that our synthetic method yielded suitable single crystals for an X-ray structural analysis.

Bartlett and his coworkers<sup>2</sup> had prepared a salt of empirical formula  $\text{F}_{17}\text{PtXe}_2$ , at the time they characterized the salt  $\text{XeF}_5^+\text{PtF}_6^-$ , and considered it likely to be  $\text{Xe}_2\text{F}_{11}^+\text{PtF}_6^-$ . The

composition of the latter, which can also be expressed as  $2\text{XeF}_6 \cdot \text{PtF}_5$  adduct, suggested that the compound  $2\text{XeF}_6 \cdot \text{SbF}_5$ , described even earlier<sup>3</sup> by Gard and Cady, was also probably an  $\text{Xe}_2\text{F}_{11}^+$  salt.

On the basis of Raman data<sup>4</sup> for  $2\text{XeF}_6 \cdot \text{AsF}_5$  and  $\text{XeF}_6 \cdot \text{AsF}_5$  and the crystal structure of  $\text{XeF}_5^+\text{AsF}_6^-$ ,<sup>5</sup> Bartlett and Wechsberg<sup>4</sup> concluded that the former complex was  $\text{Xe}_2\text{F}_{11}^+\text{AsF}_6^-$ . Although Bartlett and Wechsberg were able to obtain single crystals of the arsenic complex,<sup>4</sup> all showed

(1) K. Leary and N. Bartlett, *J. Chem. Soc., Chem. Commun.*, 903 (1972).

(2) N. Bartlett, F. Einstein, D. Stewart, and J. Trotter, *Chem. Commun.*, 550 (1966); *J. Chem. Soc. A*, 478 (1967).

(3) G. L. Gard and G. H. Cady, *Inorg. Chem.*, 3, 1945 (1964).

(4) N. Bartlett and M. Wechsberg, *Z. Anorg. Allg. Chem.*, 385, 5 (1971).

(5) N. Bartlett, B. G. DeBoer, F. J. Hollander, F. O. Sladky, D. H. Templeton, and A. Zalkin, *Inorg. Chem.*, 13, 780 (1974).

Table I. Positional and Thermal Parameters for  $\text{Xe}_2\text{F}_{11}^+\text{AuF}_6^-$ 

Atom	x	y	z	$B_{11}$	$B_{22}$	$B_{33}$	$B_{12}$	$B_{13}$	$B_{23}$
Au	0.15834 (6)	0.250 <sup>a</sup>	0.02276 (5)	2.42 (3)	3.32 (3)	3.95 (3)	0 <sup>a</sup>	-0.44 (2)	0 <sup>a</sup>
Xe(1)	0.29072 (9)	0.250 <sup>a</sup>	0.66069 (7)	2.80 (4)	4.73 (6)	3.03 (5)	0 <sup>a</sup>	0.32 (3)	0 <sup>a</sup>
Xe(2)	0.2013 (1)	0.250 <sup>a</sup>	0.38245 (7)	3.08 (4)	5.06 (6)	3.36 (5)	0 <sup>a</sup>	-0.65 (3)	0 <sup>a</sup>
F(1)	0.234 (1)	0.250 <sup>a</sup>	0.7726 (6)	7.0 (5)	7.9 (7)	2.3 (4)	0 <sup>a</sup>	1.0 (4)	0 <sup>a</sup>
F(4)	0.077 (4)	0.250 <sup>a</sup>	0.2933 (7)	6.5 (6)	11.1 (8)	5.3 (6)	0 <sup>a</sup>	-3.7 (4)	0 <sup>a</sup>
F(7)	0.2238 (8)	0.250 <sup>a</sup>	0.5254 (6)	4.4 (4)	4.8 (5)	3.7 (5)	0 <sup>a</sup>	-0.2 (4)	0 <sup>a</sup>
F(8)	0.041 (1)	0.250 <sup>a</sup>	-0.0771 (6)	4.1 (4)	8.3 (6)	5.4 (5)	0 <sup>a</sup>	-1.6 (4)	0 <sup>a</sup>
F(10)	0.270 (1)	0.250 <sup>a</sup>	0.1212 (7)	5.6 (5)	7.2 (6)	5.9 (7)	0 <sup>a</sup>	-3.2 (4)	0 <sup>a</sup>
F(11)	0.3300 (9)	0.250 <sup>a</sup>	-0.0407 (7)	3.1 (4)	9.3 (8)	6.9 (7)	0 <sup>a</sup>	1.0 (4)	0 <sup>a</sup>
F(12)	-0.0143 (9)	0.250 <sup>a</sup>	0.0857 (6)	3.1 (4)	9.9 (7)	5.5 (5)	0 <sup>a</sup>	0.6 (3)	0 <sup>a</sup>
F(2)	0.1448 (6)	0.1026 (9)	0.6578 (4)	4.3 (3)	6.1 (4)	5.3 (4)	-1.9 (3)	1.0 (2)	0.2 (3)
F(3)	0.4114 (7)	0.0949 (8)	0.7046 (4)	5.0 (3)	6.3 (4)	5.1 (4)	1.5 (3)	0.0 (2)	1.3 (3)
F(5)	0.2914 (7)	0.096 (1)	0.3168 (5)	5.9 (4)	11.3 (7)	7.0 (5)	1.7 (4)	-0.0 (3)	-4.5 (5)
F(6)	0.0708 (6)	0.1013 (8)	0.4160 (5)	3.6 (3)	5.4 (4)	8.1 (5)	-1.4 (2)	-0.9 (2)	0.1 (3)
F(9)	0.1587 (8)	0.033 (1)	0.0236 (6)	8.2 (4)	4.3 (4)	9.6 (6)	-0.2 (3)	-3.0 (4)	0.3 (4)

<sup>a</sup> Fixed parameter.

disorder or gross twinning features and were unsuitable for an X-ray structure determination. Sladky and Bartlett<sup>6</sup> had similar difficulties in preparing single crystals of  $\text{Xe}_2\text{F}_{11}^+\text{RuF}_6^-$ , which was considered to be the best platinum-metal-pentafluoride case (because of the lower atomic number of ruthenium) for a structural characterization of the cation.

The controversy concerning the nature of the bonding in  $\text{XeF}_6^{7-9}$  and the role of the "nonbonding" Xe valence electron pair in determining the shape of the molecule gives added interest to the geometry of the  $\text{Xe}_2\text{F}_{11}^+$  cation. It seemed even at the outset, however (see ref 4), that the complex cation would be a symmetrical fluorine-bridged  $\text{F}_3\text{Xe}\cdots\text{F}\cdots\text{XeF}_5$  species and, in particular, a relationship to the crystalline  $\text{XeF}_6$  structure<sup>10</sup> was anticipated.

Although the structure determination of an alkali fluoroaurate would have been more satisfactory for the description of the  $\text{AuF}_6^-$  ion, single crystals of  $\text{MAuF}_6$  (M = Cs, Rb, K, etc.) have not yet been obtained. Nevertheless, with allowance for the perturbing influence of the unsymmetrical cation, an adequate description of  $\text{AuF}_6^-$  has been provided by the structure of  $\text{Xe}_2\text{F}_{11}^+\text{AuF}_6^-$ .

### Experimental Section

**Crystal Preparation.**  $\text{Xe}_2\text{F}_{11}^+\text{AuF}_6^-$  was prepared as previously described.<sup>1</sup> Crystals were grown by placing  $\text{Xe}_2\text{F}_{11}^+\text{AuF}_6^-$  (1.28 mmol) and  $\text{XeF}_4$  (5.91 mmol), prepared as previously described,<sup>11</sup> in a Monel autoclave bomb. Fluorine gas (70 mmol) was added by condensing with liquid nitrogen. The bomb was heated at 400° for 48 hr under a fluorine pressure of 1000 psi. It was then cooled slowly to room temperature overnight and the excess  $\text{F}_2$  and  $\text{XeF}_6$  were removed under vacuum. The bomb was opened in the dry nitrogen atmosphere of a Vacuum Atmospheres Corp. Dri-lab. The  $\text{Xe}_2\text{F}_{11}^+\text{AuF}_6^-$  lay in the bottom of the bomb as a mass of small yellow-green plates, whose crystal habit was orthorhombic. Crystals were wedged into small quartz capillaries with Pyrex push rods and then sealed temporarily with Kel-F grease. On removal from the Dri-lab the capillaries were immediately sealed in a small flame. Because  $\text{Xe}_2\text{F}_{11}^+\text{AuF}_6^-$  is extremely water sensitive, the utmost precautions were taken to exclude water from all apparatus and materials.

**Crystal Data.**  $\text{F}_{11}\text{AuXe}_2$  (mol wt 782.5) is orthorhombic with

(6) N. Bartlett and F. O. Sladky, *J. Amer. Chem. Soc.*, **90**, 5316 (1968).

(7) L. S. Bartell, R. M. Gavin, Jr., H. B. Thompson, and C. L. Chernick, *J. Chem. Phys.*, **48**, 2547 (1965); K. Hedberg, S. H. Peterson, R. R. Ryan, and B. Weinstock, *ibid.*, **44**, 1726 (1966); R. M. Gavin, Jr., and L. S. Bartell, *ibid.*, **48**, 2460 (1968); L. S. Bartell and R. M. Gavin, Jr., *ibid.*, 2466 (1968).

(8) R. F. Code, W. E. Falconer, W. Klemperer, and I. Ozier, *J. Chem. Phys.*, **47**, 4955 (1967); W. E. Falconer, A. Buchler, J. L. Stauffer, and W. Klemperer, *ibid.*, **48**, 312 (1968).

(9) G. L. Goodman, *J. Chem. Phys.*, **56**, 5038 (1972).

(10) R. D. Burbank and G. R. Jones, *Science*, **168**, 248 (1970).

(11) L. V. Streng and A. G. Streng, *Inorg. Chem.*, **4**, 1370 (1965); J. H. Holloway, *Chem. Commun.*, 22 (1966); S. M. Williamson, *Inorg. Syn.*, **11**, 147 (1968).

$a = 9.115$  (6) Å,  $b = 8.542$  (25) Å,  $c = 15.726$  (20) Å,  $V = 1224.3$  Å<sup>3</sup>,  $Z = 4$ ,  $d_c = 4.24$  g cm<sup>-3</sup>,  $\mu(\text{Mo K}\alpha) = 182$  cm<sup>-1</sup>, and  $F(000) = 1345.72$ . The rather large estimated standard deviations of the cell constants reflect changes during data collection, presumably as a consequence of some decomposition. A powder photograph of the bulk material was indexed using the single-crystal unit cell dimensions. The unit cell volume satisfies Zachariason's criterion<sup>12</sup> for close-packed fluoride lattices, since the effective volume per fluorine atom is 18.0 Å<sup>3</sup>. Single-crystal Weissenberg photographs indicated that the space group was either  $Pnma$  (No. 62) or  $Pn2_1b$  (No. 33 in a nonstandard setting). The structure was successfully refined in the centrosymmetric group  $Pnma$ . Due to the extreme reactivity of the material no attempt was made to obtain an experimental density.

**X-Ray Measurements.** A Picker automatic four-circle diffractometer, equipped with a fine-focus Mo anode tube ( $\lambda(\text{Mo K}\alpha_1) = 0.70926$  Å) and a graphite monochromator, was used for data collection. Accurate cell dimensions were obtained from a least-squares refinement of the orientation matrix and of the cell parameters based on the four angle settings ( $2\theta$ ,  $\omega$ ,  $\psi$ ,  $\phi$ ) of 12 high-angle ( $45^\circ \leq 2\theta \leq 50^\circ$ ) reflections. Intensity data were collected by the  $\theta$ - $2\theta$  scan technique, at a scan rate of 2°/min. The scan width was 1.4°. Background counts were offset from the scan limits by 0.8°, and each count lasted 4 sec. Three standards were checked every 50 reflections. The temperature during data collection was  $24 \pm 1^\circ$ . Because  $\text{Xe}_2\text{F}_{11}^+$  decomposes slowly in X-rays, we had to use four crystals in the data collection. All four were flat plates, elongated along the  $b$  axis, and each was mounted with the  $b$  axis along the  $\phi$  axis of the diffractometer. The crystals had the following dimensions for the  $h$ ,  $k$ , and  $l$  directions, respectively: no. 1, 0.255, 0.345, 0.047 mm; no. 2, 0.282, 0.351, 0.060 mm; no. 3, 0.204, 0.462, 0.096 mm; no. 4, 0.231, 0.600, 0.072 mm (the precision of these measurements is probably no better than  $\pm 0.005$  mm). Each of the crystals was bounded by the six planes of the forms  $\{100\}$ ,  $\{010\}$ , and  $\{001\}$ . The first three crystals provided a complete set of  $+h, +k, +l$  data to  $2\theta \leq 50^\circ$  (1162 reflections). Crystal no. 4 yielded a complete set of  $+h, +k, +l$  and  $+h, -k, +l$  data to  $2\theta \leq 40^\circ$  (1204 reflections). A crystal was discarded when an  $\omega$ -scan half-width of any standard reflection became  $\geq 0.25^\circ$ . Intensity decay of the standards was no greater than 20.0% in any one crystal. Corrections for decay were made.

Because of the large absorption coefficient (182 cm<sup>-1</sup>) and the fact that all the crystals were much larger than the optimum size, the data were corrected for absorption using a program developed by Coppens, Leiserowitz, and Rabinovich,<sup>13</sup> modified by Cahen and Ibers<sup>14,15</sup> and adapted for local use. This method incorporates numerical integration using a gaussian grid. The data were treated and weights assigned as previously described<sup>16</sup> with the exception that a  $q$  factor (used to decrease the weights of large intensities) of zero was used. Scattering factors<sup>17</sup> for neutral gold, xenon, and fluorine

(12) W. H. Zachariason, *J. Amer. Chem. Soc.*, **70**, 2147 (1948).

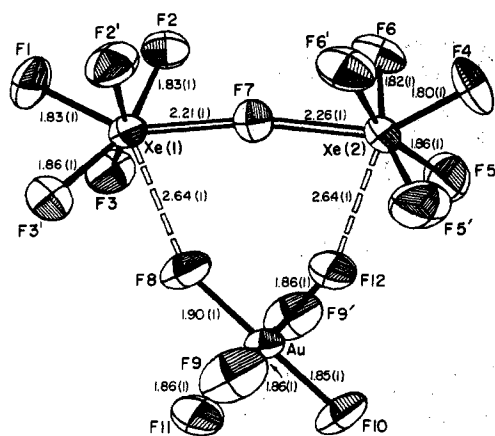
(13) P. Coppens, L. Leiserowitz, and D. Rabinovich, *Acta Crystallogr.*, **18**, 1035 (1965).

(14) J. A. Ibers and D. Cahen, private communication to A. Zalkin.

(15) D. Cahen and J. A. Ibers, *J. Appl. Crystallogr.*, **5**, 398 (1972).

(16) D. D. Gibling, C. J. Adams, M. Fischer, A. Zalkin, and N. Bartlett, *Inorg. Chem.*, **11**, 2325 (1972).

(17) P. A. Doyle and P. S. Turner, *Acta Crystallogr., Sect. A*, **24**, 390 (1968).

Figure 1. The structural unit  $\text{Xe}_2\text{F}_{11}^+\text{AuF}_6^-$ .Table III. Interatomic Distances (Å) and Angles (deg) for  $\text{Xe}_2\text{F}_{11}^+\text{AuF}_6^-$ <sup>a</sup>

Anion		Ionic Angles			
F9-Au-F9'	179.1 (3)	F1-Xe1-F2	79.6 (4)	F4-Xe2-F6	79.4 (4)
F8	90.4 (4)	F3	79.0 (4)	F5	81.1 (5)
F8-Au-F11	91.6 (6)	F2-Xe1-F2	86.8 (3)	F6-Xe2-F6	88.6 (3)
F12	88.0 (5)	F3	87.1 (4)	F5	87.4 (6)
F10-Au-F11	89.2 (5)	F3-Xe1-F3	91.1 (3)	F5-Xe2-F5	89.9 (3)
F12	91.2 (6)	Xe2-F7-Xe1	169.2 (2)		
		Interionic Distances and Angles			
Xe1-F8	2.64 (1)	F1-Xe1-F7	147.6 (6)	F4-Xe2-F7	146.3 (7)
F9	3.27 (1)	F8	136.3 (6)	F12	139.8 (7)
Xe2-F12	2.64 (1)	F9	132.2 (3)	F9	135.9 (2)
F9	3.52 (1)				

<sup>a</sup> Estimated standard deviations are in parentheses.Table IV. Raman Spectra of  $\text{Xe}_2\text{F}_{11}^+$  Salts and Related Species (Shifts in  $\text{cm}^{-1}$ )

$\text{IF}_6^-$ <sup>a</sup>	$(\text{NO}^+)_2\text{PdF}_6^{2-}$	$(\text{XeF}_5^+)_2\text{PdF}_6^{2-}$ <sup>b</sup>	$(\text{Xe}_2\text{F}_{11}^+)_2\text{PdF}_6^{2-}$	$(\text{Xe}_2\text{F}_{11}^+)\text{AuF}_6^-$	$\text{Cs}^+\text{AuF}_6^-$
710 ( $\nu_1$ ) vs		653 s	{ 668 w 651 vs	661 s	
631 ( $\nu_7$ ) sh		634 vw	630 m	640 w	
614 ( $\nu_2$ ) vs		{ 616 vw 606 w	{ 615 w 610 m 606 w	{ 626 w 600 s	
602 ( $\nu_4$ ) sh		590 ms	{ 591 s 583 m 568 s	595 vs 590 vs	595 ( $\nu_1$ ) vs
	573 ( $\nu_1$ ) s	558 ms	568 s		
	554 ( $\nu_2$ ) ms	535 s	546 w		
					530 ( $\nu_2$ ) vw
370 ( $\nu_8$ ) w		{ 425 vw 396 vw	{ 412 vw 396 vw	400 w	
318 ( $\nu_3$ ) m		309 w	296 w, b	356 w 290 w	
274 ( $\nu_6$ ) w		269 w	270 w, b	...	
	243 ( $\nu_5$ ) ms	245 w	245 w, b		
				221 m	224 ( $\nu_3$ ) s

<sup>a</sup> L. E. Alexander and I. R. Beattie, *J. Chem. Soc. A*, 3091 (1971). <sup>b</sup> N. Bartlett, K. Leary, D. H. Templeton, and A. Zalkin, *Inorg. Chem.*, 12, 1726 (1973).

were used. Values for anomalous dispersion,  $\Delta f'$  and  $\Delta f''$ , were taken from Cromer and Liberman.<sup>18</sup>

**Structure Refinement.** Initially, the structure was solved using the data from crystal no. 4 only ( $2\theta < 40^\circ$ ). This set of data yielded an averaged set of 633 unique reflections, of which 529 satisfying the condition  $I \geq 3\sigma(I)$  were used in the least-squares refinement.

A Patterson function yielded the positions of the two Xe and one Au atoms and refined to  $R = 0.21$ . The Patterson map confirmed the choice of the centric space group since all the Harker sections had either  $y = 0$  or  $y = 1/2$ . A difference Fourier based on the set of phases generated by the least-squares refinement gave the positions of all of the fluorine atoms. Least-squares refinement incorporating

anisotropic temperature factors for all atoms gave a final  $R$  factor of 0.04, using the data from crystal no. 4.

The data obtained from the first three crystals ( $+h, +k, +l$ ,  $2\theta < 50^\circ$ ) were then scaled and averaged with the set obtained from crystal no. 4. Of the 1162 total independent data, the 874 which satisfied the condition  $I \geq 3\sigma(I)$  were used for the least-squares refinement. A least-squares refinement using the combined data gave  $R = 4.48\%$  and weighted  $R_w = 3.98\%$ .

It was noted that the higher angle data ( $40^\circ \leq 2\theta \leq 50^\circ$ ) had large weighted discrepancies,  $w(\Delta F)^2$ . These data had been measured only once whereas the data below  $2\theta = 40^\circ$  were measured at least three times. For multiply measured data, the estimated standard deviation is based on the larger of either their counting statistics or their scatter, and thus the standard deviations of the high-angle data were consequently smaller. To correct this situation a minimum value corresponding to what was observed for the weaker lower angle data was then applied as a lower limit to the standard deviations of the higher angle data. The four sets of data were rescaled. All of the data with  $(\sin \theta)/\lambda < 0.15$  (a total of 22 reflections) were arbitrarily deleted because of excessively large discrepancies; this is no doubt

due to the inadequacies of the absorption correction. Examination of the data showed no extinction effects.

The final least-squares refinement, with all atoms anisotropic, gave an  $R$  factor of 0.052 for all 1140 reflections, and 0.036 for the 862 ( $I \geq 3\sigma(I)$ ) nonzero weighted reflections. The weighted  $R_w$  was 0.025. The standard deviation of an observation of unit weight was 1.36. The largest shift of any parameter divided by its estimated standard deviation on the last cycle of least-squares was  $\leq 0.0012$ .

A final difference Fourier showed that the largest residual electron density was  $1.91 \text{ e}/\text{Å}^3$  near the gold atom. Table I gives the positional and thermal parameters from the final refinement. Observed structure factors, standard deviations and differences are given in Table II.<sup>19</sup> Table III gives chemically significant distances and angles.

(18) D. T. Cromer and D. Liberman, *J. Chem. Phys.*, 53, 1891 (1970).

(19) See paragraph at end of paper regarding supplementary material.

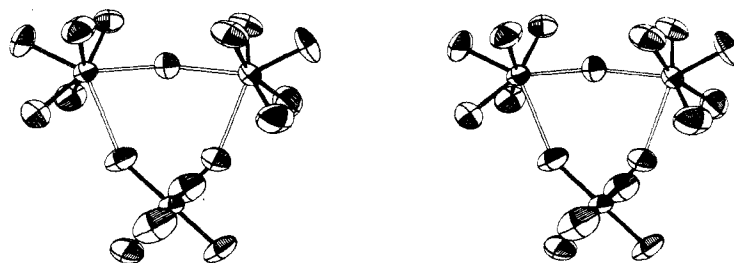


Figure 2. Stereogram of the  $\text{Xe}_2\text{F}_{11}^+\text{AuF}_6^-$  structure unit.

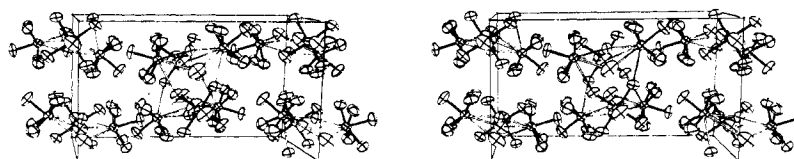


Figure 3. Stereogram showing the arrangement of the  $\text{Xe}_2\text{F}_{11}^+\text{AuF}_6^-$  units in the unit cell (view along the  $b$  axis).

**Raman Spectra.** Microcrystalline samples of  $[\text{XeF}_5^+]_2\text{PdF}_6^{2-}$ ,  $[\text{Xe}_2\text{F}_{11}^+]_2\text{PdF}_6^{2-}$ ,  $\text{Xe}_2\text{F}_{11}^+\text{AuF}_6^-$ , and  $\text{XeF}_5^+\text{AuF}_6^-$ , enclosed in 1-mm o.d. quartz capillaries, were excited at 6328 Å, using a 100-mW He-Ne ion laser, and spectra were recorded from a Spex Model 1400 double monochromator. Spectra were also obtained on a Cary 83 spectrometer equipped with a 100-mW  $\text{Ar}^+$  ion (4880-Å) laser. The spectra are tabulated in Table IV and the  $\text{AuF}_6^-$  salt spectra are given in Figure 6.<sup>19</sup>

### Description of the Structure

As may be seen from Figures 1-3 and Table III, the structure analysis clearly defines an  $\text{AuF}_6^-$  group and a  $\text{Xe}_2\text{F}_{11}^+$  group. The latter consists of two similar  $\text{XeF}_5^+$  groups linked by an additional common F atom. All of these groups ( $\text{AuF}_6^-$ ,  $\text{Xe}_2\text{F}_{11}^+$  and its  $\text{XeF}_5^+$  components) possess mirror symmetry.

The  $\text{AuF}_6^-$  group is approximately octahedral, with only one Au-F interatomic distance ( $\text{Au}-\text{F}_8 = 1.90(1) \text{ \AA}$ ) departing significantly from the average value of  $1.86(1) \text{ \AA}$ . The cis F-Au-F angles are close to  $90^\circ$ , the greatest deviation being for  $\text{F}_8-\text{Au}-\text{F}_{12} = 88.0(5)^\circ$ .

Each  $\text{XeF}_5^+$  group of the  $\text{Xe}_2\text{F}_{11}^+$  species approximates to a square-based pyramid, with the xenon atom placed below the base. The  $\text{F}_{\text{ax}}-\text{Xe}-\text{F}_{\text{eq}}$  angles are  $\sim 80^\circ$  in both  $\text{XeF}_5^+$  groups. On the other hand, each of the groups departs significantly from  $C_{4v}$  symmetry and the cis  $\text{F}_{\text{eq}}-\text{Xe}-\text{F}_{\text{eq}}$  angles in each group are not equivalent. The greatest cis angle of each  $\text{XeF}_5^+$  equatorial set is that furthest from the atom (F7) which links the  $\text{XeF}_5^+$  groups to define the  $\text{Xe}_2\text{F}_{11}^+$  species. Coincidentally, the greatest cis equatorial angles in each  $\text{XeF}_5^+$  group are also associated with the longest Xe-F distances within the group.

Although the interatomic distances  $\text{Xe}1-\text{F}7$  and  $\text{Xe}2-\text{F}7$  are sufficiently short [2.21(1) and 2.26(1), respectively] to warrant the identification of an  $\text{Xe}_2\text{F}_{11}^+$  group, all other intergroup contacts are sufficiently long that they may be classified as van der Waals contacts. The  $\text{Xe}1-\text{F}7-\text{Xe}2$  angle is not quite linear [ $169.2(2)^\circ$ ]. The F7-Xe distances are not significantly different and indeed the entire  $\text{Xe}_2\text{F}_{11}^+$  group has essentially  $C_{2v}$  symmetry.

The bridging F atom (F7) is not the only F atom of interest in relationship to the  $\text{XeF}_5^+$  groups. It is seen that each Xe atom of each  $\text{XeF}_5^+$  is approached by three other F atoms (of neighboring  $\text{AuF}_6^-$  groups) as well as by F7. Thus Xe1 is associated with F7, F9, F9', and F8 and Xe2 with F7, F9, F9', and F12 (see Figure 3). These sets of four F atoms are arranged about the base of the approximately square-pyramidal  $\text{XeF}_5^+$  groups, such that, together with the F atoms of

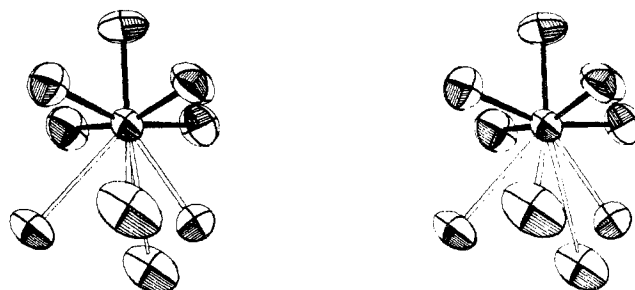


Figure 4. Stereogram showing the typical Xe coordination in F atoms (exemplified by Xe(1) coordination).

the  $\text{XeF}_5^+$ , they form a distorted capped archimedean anti-prism arrangement. The arrangement is illustrated, for the Xe1 case, in Figure 4.

### Discussion

Prior to the structure determination, chemical, vibrational, spectroscopic, and Mossbauer evidence<sup>1</sup> had indicated the formulation  $\text{Xe}_2\text{F}_{11}^+\text{AuF}_6^-$  for the  $\text{F}_{17}\text{Xe}_2\text{Au}$  material. The X-ray structure is fully compatible with that formulation.

The geometry of the  $\text{AuF}_6^-$  ion is defined for the first time in this structure. A low-spin  $d_{12g}^6$   $\text{Au(V)}$  electron configuration is anticipated to be akin to the configurations of  $\text{Pt(IV)}$  and  $\text{Pd(IV)}$  and like them to favor a regular octahedral  $\text{MF}_6^-$  species. Any departures from octahedral symmetry, in this structure, can be excused on the basis of possible distorting influences of the  $\text{Xe}_2\text{F}_{11}^+$  cation which is far from octahedral symmetry itself. The average Au-F anion interatomic distance of  $1.86(1) \text{ \AA}$  compares with the average Pt-F distance<sup>2</sup> of  $1.89(5) \text{ \AA}$  for  $\text{PtF}_6^-$  in  $\text{XeF}_5^+\text{PtF}_6^-$ . The greater nuclear charge of Au relative to Pt is anticipated<sup>20</sup> to result in a shorter M-F bond in the Au case.

This structure is at least of as much interest for its cation as for its anion. To a first approximation the complex cation has the form anticipated for an assembly of two  $\text{XeF}_5^+$  ions and a common  $\text{F}^-$ . Thus the geometry of each  $\text{XeF}_5^+$  component resembles that of  $\text{XeF}_5^+$ <sup>21</sup> and the coordination of each Xe atom (represented in Figure 4) closely resembles that for Xe in  $\text{XeF}_5^+\text{RuF}_6^-$ . A comparison of the geometry

(20) N. Bartlett, *Angew. Chem., Int. Ed. Engl.*, 7, 433 (1968).

(21) N. Bartlett, K. Leary, D. H. Templeton, and A. Zalkin, *Inorg. Chem.*, 12, 1726 (1973).

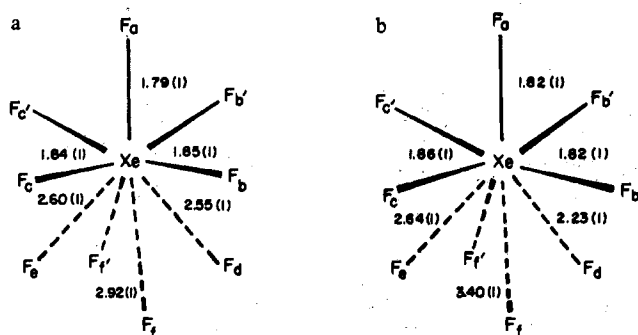


Figure 5. (a)  $\text{XeF}_5^+$  in  $\text{XeF}_5^+\text{RuF}_6^{2-}$  and (b) the  $\text{XeF}_5$  unit (average) in  $\text{Xe}_2\text{F}_{11}^+\text{AuF}_6^-$ .

	a	b
$\text{F}_{\text{eq}}\text{-Xe-F}_{\text{ax}}$	79.0 (2)°	79.9 (2)°
$\text{F}_b\text{-Xe-F}_b'$	87.8 (2)°	87.7 (2)°
$\text{F}_c\text{-Xe-F}_c'$	87.0 (2)°	90.5 (2)°
$\text{F}_b\text{-Xe-F}_c$	88.4 (4)°	87.2 (3)°
$\text{F}_d\text{-Xe-F}_a$	142.3 (7)°	147.0 (5)°
$\text{F}_e\text{-Xe-F}_a$	140.6 (6)°	138.0 (5)°
$\text{F}_f\text{-Xe-F}_a$	129.6 (3)°	134.0 (2)°

of the  $\text{XeF}_5$  unit in  $\text{Xe}_2\text{F}_{11}^+$  with that of the  $\text{XeF}_5^+$  cation in  $\text{XeF}_5^+\text{RuF}_6^-$  is given in Figure 5. The close approach of F7 to each Xe atom and the departure of the Xe-F-Xe angle from linearity suggest that a measure of covalency should be incorporated into any bonding description. Nevertheless, the ionic model  $\text{XeF}_5^+\text{F}^-\text{XeF}_5^+$  accounts for a number of the observed structural features of  $\text{Xe}_2\text{F}_{11}^+$ . In previous papers<sup>21,22</sup> we have argued for steric activity of the nonbonding Xe(VI) electron pair in the pseudooctahedral  $\text{XeF}_5^+$  species. We can allow that the close approach of  $\text{F}^-$  to  $\text{XeF}_5^+$  would deflect the nonbonding valence electron pair from its axial position toward the bisectors of the  $\text{F3-Xe1-F3}'$  and the  $\text{F5-Xe2-F5}'$  angles. Increase in the nonbonding pair repulsive interactions with the  $\text{Xe1-F3}$  and  $\text{Xe2-F5}$  bonds, consequent upon such deflection of the electron pairs, could also account for the lengthening of the  $\text{Xe1-F3}$  and  $\text{Xe2-F5}$  interatomic distances. Similarly, the deflection of the Xe(VI) "pairs" could account for shortening of the  $\text{Xe1-F2}$  and

$\text{Xe2-F6}$  distances. In  $\text{XeF}_5^+$  the Xe-F equatorial distances<sup>21</sup> are 1.84 Å.

As may be seen from the Raman data given in Table IV, the complex  $4\text{XeF}_6 \cdot \text{PdF}_4$ <sup>23</sup> contains essentially the same cation as  $\text{Xe}_2\text{F}_{11}^+\text{AuF}_6^-$  and may, therefore, be confidently formulated as  $[\text{Xe}_2\text{F}_{11}^+]_2\text{PdF}_6^{2-}$ . The F bridging of two  $\text{XeF}_5$  groups in the  $\text{Xe}_2\text{F}_{11}^+$  cation appears to be characterized by a "bridge stretch" at  $\sim 360 \text{ cm}^{-1}$ ; but, in keeping with the observed structure, the complex cation otherwise behaves vibrationally like two weakly coupled  $\text{XeF}_5^+$  species.

Since crystalline  $\text{XeF}_6$  can be described<sup>10</sup> as  $\text{XeF}_5^+\text{F}^-$  (clustered either in tetramers or hexamers) it is not surprising that  $\text{Xe}_2\text{F}_{11}^+$  looks like a fragment of an  $\text{XeF}_6$  tetramer or hexamer. The resemblance is closest to the tetramer. In a bonding description of  $\text{Xe}_2\text{F}_{11}^+$  and crystalline  $\text{XeF}_6$ ,  $\text{XeF}_5^+$  and  $\text{F}^-$  are clearly important contributing canonical forms. Perhaps the best description of  $\text{Xe}_2\text{F}_{11}^+$  is as a resonance hybrid of  $(\text{XeF}_5^+\text{F}^-\text{XeF}_5^+)$ ,  $(\text{XeF}_6\text{XeF}_5^+)$ , and  $(\text{XeF}_5^+\text{XeF}_6)$  with the first canonical form dominant.

It seems probable that all  $\text{XeF}_6$  complexes with fluoride ion acceptors will prove to be either  $\text{XeF}_5^+$  or  $\text{Xe}_2\text{F}_{11}^+$  salts. In particular, the  $2\text{XeF}_6 \cdot \text{MF}_5$  and  $4\text{XeF}_6 \cdot \text{MF}_4$  complexes reported by Cady and his coworkers<sup>3,24</sup> are very probably  $\text{Xe}_2\text{F}_{11}^+$  salts.

**Acknowledgment.** This work was supported by the U. S. Atomic Energy Commission and the Committee on Research, University of California, Berkeley, Calif.

**Registry No.**  $\text{Xe}_2\text{F}_{11}^+\text{AuF}_6^-$ , 39043-77-1.

**Supplementary Material Available.** Table II, a listing of structure factor amplitudes, and Figure 6, showing the Raman spectra of some  $\text{AuF}_6^-$  salts, will appear following these pages in the microfilm edition of this volume of the journal. Photocopies of the supplementary material from this paper only or microfiche (105 × 148 mm, 24× reduction, negatives) containing all of the supplementary material for the papers in this issue may be obtained from the Journals Department, American Chemical Society, 1155 16th St., N.W., Washington, D. C. 20036. Remit check or money order for \$3.00 for photocopy or \$2.00 for microfiche, referring to code number INORG-74-775.

(23) K. Leary and N. Bartlett, to be submitted for publication.

(24) K. E. Pullen and G. H. Cady, *Inorg. Chem.*, **5**, 2077 (1966); **6**, 1300, 2267 (1967).

(22) N. Bartlett, M. Gennis, D. D. Gibler, B. K. Morrell, and A. Zalkin, *Inorg. Chem.*, **12**, 1717 (1973).